

# Reducing CO2 footprint through synergies in carbon free energy vectors and low carbon fuels

Wang, W., Herreros, J. M., Tsolakis, A., York, A. P. E.

Author post-print (accepted) deposited by Coventry University's Repository

**Original citation & hyperlink:**

Wang, W, Herreros, JM, Tsolakis, A & York, APE 2016, 'Reducing CO2 footprint through synergies in carbon free energy vectors and low carbon fuels' Energy, vol 112, pp. 976-983. DOI: 10.1016/j.energy.2016.07.010  
<https://dx.doi.org/10.1016/j.energy.2016.07.010>

DOI 10.1016/j.energy.2016.07.010

ISSN 0360-5442

ESSN 1873-6785

Publisher: Elsevier

***NOTICE: this is the author's version of a work that was accepted for publication in Energy. Changes resulting from the publishing process, such as peer review, editing, corrections, structural formatting, and other quality control mechanisms may not be reflected in this document. Changes may have been made to this work since it was submitted for publication. A definitive version was subsequently published in Energy VOL 112, (2016) DOI: 10.1016/j.energy.2016.07.010***

**© 2016, Elsevier. Licensed under the Creative Commons Attribution-NonCommercial-NoDerivatives 4.0 International**

<http://creativecommons.org/licenses/by-nc-nd/4.0/>

Copyright © and Moral Rights are retained by the author(s) and/ or other copyright owners. A copy can be downloaded for personal non-commercial research or study, without prior permission or charge. This item cannot be reproduced or quoted extensively from without first obtaining permission in writing from the copyright holder(s). The content must not be changed in any way or sold commercially in any format or medium without the formal permission of the copyright holders.

This document is the author's post-print version, incorporating any revisions agreed during the peer-review process. Some differences between the published version and this version may remain and you are advised to consult the published version if you wish to cite from it.

# 1 Reducing CO<sub>2</sub> footprint through synergies in Carbon Free Energy Vectors and Low Carbon 2 Fuels

3 W. Wang<sup>a</sup>, J.M. Herreros<sup>a</sup>, A. Tsolakis<sup>a\*</sup> and A.P.E. York<sup>b</sup>

4 <sup>a</sup>*School of Mechanical Engineering, University of Birmingham, Edgbaston, B15 2TT, UK*

5 <sup>b</sup>*Johnson Matthey Technology Centre, Blount's Court, Sonning Common, Reading RG4 9NH, UK*

6 \* *Corresponding author. tel.: +44 (0) 121 414 4170, fax: +44 (0) 121 414 7484; a.tsolakis@bham.ac.uk*

## 7 Abstract

8 Carbon-footprint from transport and power generation can significantly be improved when  
9 carbon free or reduced carbon energy carriers are utilised that are compatible with the current  
10 technology of the internal combustion (IC) engines. The current study focuses on the reduction of  
11 diesel engine CO<sub>2</sub> emissions by improving ammonia and hydrogen combustion through the  
12 incorporation of alternative fuel, diethyl glycol diethyl ether (DGE) as an oxygenated fuel blend and  
13 combustion enhancer. The aim of the work is to study the potential synergies between DGE and two  
14 carbon free energy vectors H<sub>2</sub> and NH<sub>3</sub> in reducing the environmental effects and contribute in  
15 decarbonising internal combustion engines. DGE's ignition properties (i.e. high cetane number)  
16 improved the H<sub>2</sub> and NH<sub>3</sub> combustion efficiencies via counteracting their high auto-ignition  
17 resistances, and also contributing in lowering the unburnt H<sub>2</sub> and NH<sub>3</sub> emissions to the atmosphere.  
18 This led in the reduction of CO<sub>2</sub> by up 50% when 60-70% of diesel fuel is replaced with DGE, H<sub>2</sub> and  
19 NH<sub>3</sub>. Synergetic effects were also found between DGE and the gaseous fuels (i.e. hydrogen and  
20 ammonia) simultaneously decreasing the levels of PM, NO<sub>x</sub>, HC and CO emitted to the atmosphere;  
21 thus mitigating the health and environmental hazards associated to diesel engines.

22 **Keywords:** DGE, hydrogen, ammonia, pollutants, emission control

## 23 1. Introduction

24 Current worldwide transportation relies primarily on fossil fuels. Effective decarbonisation of the  
25 energy sector and especially transportation can be achieved by adopting fuel substitution with an  
26 energy carrier free of carbon. Ammonia (NH<sub>3</sub>) and hydrogen (H<sub>2</sub>) can be renewably resourced by  
27 utilising solar and wind energy. Hydrogen is believed to be one of the most potential alternatives [1]  
28 but due to its low volumetric energy density and infrastructure challenges associated with its  
29 transportation and handling, H<sub>2</sub> powered vehicles are still a niche product and widespread use is a

30 long term goal [2].

31 Ammonia has been studied as an energy [3] and hydrogen carrier for fuel cells [4, 5] and IC  
32 engines, providing that there is a process to split the  $\text{NH}_3$  into  $\text{N}_2$  and  $\text{H}_2$  [6]. In recent work we have  
33 proposed that this is feasible through the application of the catalytic ammonia reforming and  
34 decomposition using the heat of the engine exhaust gas to drive the reactions [2]. The combustion of  
35 reformed gas, i.e.  $\text{H}_2$ ,  $\text{N}_2$ ,  $\text{H}_2\text{O}$  and unconverted  $\text{NH}_3$ , in diesel engine with diesel fuels has shown to  
36 reduce carbonaceous emissions, including  $\text{CO}_2$ . However, under a range of engine operating  
37 conditions, higher  $\text{NO}_x$  emissions and incomplete combustion of the reformed gas was seen, similarly  
38 to LPG-diesel and natural gas-diesel dual fueled combustion, causing the production of other  
39 undesired emissions such as  $\text{NH}_3$  slippage [7]. Combustion improvements were observed in a study of  
40 LPG-diesel and CNG-diesel fueled diesel engine with the use of a high cetane number fuel, such as  
41 diethyl ether (DEE, CN >125) [8, 9]. Most recently, Ryu et al. [10] investigated the compression  
42 ignition combustion of ammonia and dimethyl ether (DME, CN = 60), where several appropriate  
43 strategies and fuel/gas mixtures were shown for the use of ammonia in direct-injection  
44 compression-ignition engines. Apart from that, DME is also referred as a cetane enhancer blended  
45 with different fuels/fuel mixtures for the purpose of particulate emission [11].

46 Similarly, diethyl glycol diethyl ether (DGE) can be regarded as another potential combustion  
47 enhancer based on its high cetane (CN = 140) number and its high content of fuel-born oxygen.  
48 Because of its featured high ignitability, DGE combustion in a diesel engine has a shorter ignition  
49 delay and was demonstrated to burn sufficiently in low-temperature combustion regime under  
50 charge-gas dilution and cooling [12]. All these characteristics of DGE can lead to the engine out  
51 improved  $\text{NO}_x$ /soot trade-off when it combusted with diesel fuel. Also as being similar to DEE, its  
52 presence (as fuel or fuel blend) in CI type of combustion is thought to be capable to assist the  
53 combustion of those less ignitable fuel alternatives, such as  $\text{H}_2$  and  $\text{NH}_3$ .

54 In this work the impact of  $\text{NH}_3$  and  $\text{H}_2$  combustion on the  $\text{CO}_2$  footprints of a diesel engine was  
55 studied. Following that, the addition of reduced carbon fuel, named DGE at different amounts into  
56 diesel, was studied as combustion improver of the carbon free gaseous fuels. The improvement in the  
57 properties of the diesel fuel (i.e. cetane number, ignition properties and presence of oxygen content)  
58 on the combustion and emission characteristics of the fuel mixture was assessed and compared in  
59 order to identify potential  $\text{CO}_2$  and other environmental benefits.

## 60        **2. Experimental**

61        *Test rig setup:* The NH<sub>3</sub> reformat was simulated using NH<sub>3</sub> and H<sub>2</sub> gas bottles, whose flows  
62 were regulated by means of flow meters. The simulated gas additions were sent into the engine intake  
63 and premixed with the intake air. The liquid fuel (pure diesel or DGE blend) was injected into the  
64 cylinder to initiate the combustion. This approach required no modification to the fuel injection  
65 system. A Thring Titan thyristor-type DC electric dynamometer was used to motor and load the  
66 engine.

67        *Test engine:* The engine is a single-cylinder, direct injection, naturally aspirated diesel engine.  
68 The main engine specifications are: bore 98.4 mm, stroke 101.6 mm, conrod length 165.0 mm,  
69 displacement volume 773 cm<sup>3</sup>, compression ratio 15.5, maximum power 8.6 kW at 2500 rpm and  
70 maximum torque 39.2 Nm at 1800 rpm.

71        *Data acquisition:* The data acquisition and combustion analysis were carried out using in-house  
72 (University of Birmingham) developed Labview software. Output from the analysis of engine cycles  
73 included the in-cylinder pressure and rate of heat release (ROHR) at varying crank angle degrees,  
74 indicated mean effective pressure (IMEP), percentage coefficient of variation (COV) of IMEP values  
75 and other combustion characteristics.

76        *Emission analysis:* The gaseous emissions including NO, NO<sub>2</sub>, N<sub>2</sub>O, CO, CO<sub>2</sub>, THC (C<sub>1</sub> based)  
77 and NH<sub>3</sub> were carried out by a MKS MultiGAS 2030 FTIR analyser (Fourier Transform Infrared  
78 Spectroscopy). Detection limits are 3.6 ppm for NO, 1.2 ppm for CO and lower than 1 ppm for the  
79 rest of gaseous species. Confidence intervals calculated using a 95% confidence level which reflects the  
80 reliability and repeatability of the equipment are shown in the results. FTIR results have been verified  
81 using known concentrations of CO<sub>2</sub>, CO, NO, NH<sub>3</sub> and THC and a Horiba MEXA 7100DEGR (CO<sub>2</sub>  
82 and CO by Non-Dispersive Infrared, oxygen (O<sub>2</sub>) by magnetopneumatic method, NO by  
83 Chemiluminescence Detection and HC by Flame Ionisation Detector) gas analyser was used to  
84 remove experimental bias during this procedure. Good agreement was obtained for the species and  
85 emission levels shown in this investigation. The hydrogen concentration in the exhaust was measured  
86 using a Hewlett Packard 5890 II gas chromatograph (GC) with thermal conductivity detector (TCD)  
87 using argon as carrier gas. An investigation of particulate matter (PM) was carried out using a TSI  
88 scanning mobility particle sizer (SMPS) 3080 electrostatic classifier to measure the particle size  
89 distribution. The sample was thermo-diluted using a rotating disk, with the dilution ratio set to 200:1

90 at 150 °C. Particulate measurement is focus on small particulates (in the range from 10 to 400 nm)  
91 being more dangerous for the environment and human health due to their higher reactivity, suspension  
92 time in the atmosphere and alveolar deposition fraction (especially ultrafine particulates lower than  
93 100 nm).

94 *Liquid fuel:* Ultra-low sulphur diesel (ULSD) fuel was used as the primary liquid fuel for  
95 baseline operation. DGE was mixed volumetrically into the diesel to obtain the desired blends. Two  
96 blends with volumetric concentrations of 20 and 40% of DGE (DGE20 and DGE40 accordingly) were  
97 selected. This allowed a comparison between 3 different CN ratings and fuel-born oxygen contents.  
98 The fuel properties are listed in Table 1 for each tested fuel/fuel blend.

99 *Test combinations of gaseous additions:* In a previous on-board ammonia dissociation study  
100 using catalytic reforming technology [2], various amounts of hydrogen flow rates were produced  
101 under different reactor conditions. Unconverted NH<sub>3</sub>, N<sub>2</sub> and H<sub>2</sub>O (no NO<sub>x</sub> production) make up the  
102 rest of the reactor product gas. For the purpose of current study, only H<sub>2</sub> and NH<sub>3</sub> were considered as  
103 the effective (combustible) reforming products; the obtained volumetric H<sub>2</sub> to reformat (H<sub>2</sub> + NH<sub>3</sub>)  
104 ratio was ranging from 0.5 to 0.9, with roughly an increase of 0.1 from one reforming condition to  
105 another. Hence to simulate the reformat gas at higher flow rate, the observed H<sub>2</sub>/reformat ratio was  
106 applied. The H<sub>2</sub> flows were chosen at 10, 15 and 20 l/min with various amounts of NH<sub>3</sub> selected  
107 accordingly to meet the actual H<sub>2</sub>/reformat ratios. Pure forms of H<sub>2</sub> and NH<sub>3</sub> were also adopted for  
108 comparison purpose. All the H<sub>2</sub>-NH<sub>3</sub> combinations are listed in Table 2.

109 *Test procedures:* The experimental runs were carried out in three separate sets for diesel and two  
110 DGE blends i.e. DGE20 and DGE40. All tests were performed under steady – state conditions at a  
111 controlled engine speed of 1500 rpm and a constant engine load of 5 bar IMEP throughout  
112 representing about 65% of full engine load at this engine speed. In all test sets, the liquid fuel blend  
113 was used to start and warm up the engine. Then different flows of NH<sub>3</sub> and H<sub>2</sub> or both combined were  
114 added into the air intake. The amount of liquid fuel injection was modified accordingly after the  
115 gaseous additions to keep the engine running at the same load. At least 20 minutes was allowed in  
116 each run for stabilising the engine before any of the readings being taken.

### 117 **3. Results and discussion**

#### 118 Liquid fuel replacement

119 The liquid fuel replacements on mass bases by the same quantity of gaseous fuels was higher in  
120 the case of diesel fuel when compared to DGE-diesel blends as shown in Figure 1. As the DGE  
121 content in the fuel blends was increased the amount of liquid fuel being replaced was reduced. This  
122 was due to the lower LHV (i.e. higher fuel-born oxygen content, Table 1) of DGE than that of diesel  
123 which increased the amount of DGE blend to keep the same engine load.

#### 124 Combustion characteristics

125 The in-cylinder pressure and rate of heat release (ROHR) of diesel and diesel-DGE blends with  
126 different gaseous additions are plotted in Figure 2a and b. While the addition of NH<sub>3</sub> (14 l/min)  
127 prolonged the ignition delay in diesel combustion (Figure 2a), the DGE's high ignitability (see Table 1)  
128 balances out the NH<sub>3</sub>'s properties of high auto-ignition temperature (651°C) and octane rating (120) [10]  
129 as can be observed by the advanced start of the combustion. It is suggested that the NH<sub>3</sub>/air  
130 pre-mixture being carried into the liquid fuel (diesel-DGE) spray periphery. When the liquid fuel  
131 ignited, a flame was propagated to initiate the combustion of the mixture (premixed  
132 DGE/diesel/NH<sub>3</sub>/air) [9]. The beneficial effects of the oxygen content in DGE molecule could partially  
133 compensate the effects of the reduction in the overall air/fuel ratio due to the oxygen dilution (decrease in  
134 the intake air) from the incorporation of gaseous fuels at the air intake. By increasing the local  
135 oxygen/fuel ratio the oxidation of the gas/fuel mixture was also facilitated. In addition, the DGE's  
136 lower compressibility than diesel (usually inverse to density, see Table 1) could result in advanced  
137 fuel injection and ignition that in turn benefits also the NH<sub>3</sub> ignition.

138 In the case of hydrogen addition, its high auto-ignition temperature and poor cetane rating did not  
139 retard the start of combustion and that was the case in presence or not of ammonia (Figure 2). This is  
140 due to the low ignition energy requirement for hydrogen (0.02 MJ/kg at stoichiometric H<sub>2</sub>/air mixture)  
141 being even lower than for many of the hydrocarbon components of the fuels [13, 14].

142 In terms of the ROHR patterns, the combustion of the diesel-NH<sub>3</sub> mixture intensified the  
143 premixed phase and resulted in shorter combustion duration compared to diesel only combustion. This  
144 was suggested to be due to the combustion of NH<sub>3</sub> and a high proportion of diesel in the premixed  
145 combustion (because of the longer available time to mix air, NH<sub>3</sub> and the liquid diesel). On the other  
146 hand, can be suggested that hydrogen's higher flame speed [15, 16] when compared to diesel and NH<sub>3</sub>  
147 led to faster and shorter combustion duration as can be seen by the larger increase in ROHR observed.  
148 The addition of DGE in diesel reduced the premixed combustion phase for the two DGE-diesel fuel

149 blends. This was due to the DGE's much higher cetane number (140) compared to that of diesel (53.9).  
150 As the DGE content increased, the ignition delay time was reduced and therefore suppressed the rate  
151 of heat release in premixed combustion.

152 Compared to the diesel baseline, the presence of the combined  $\text{NH}_3$  and  $\text{H}_2$  also intensified  
153 premixed combustion due to the rapid burning of  $\text{H}_2$  which thermally favoured the ignition and  
154 combustion velocity of  $\text{NH}_3$  [17] and/or even decompose  $\text{NH}_3$  into  $\text{H}_2$  and  $\text{N}_2$  [18]. These effects  
155 contributed to the largely increased peak ROHR and hence the in-cylinder temperature (reflected by  
156 the increased cylinder pressure) and shortened the overall combustion duration. The presence of DGE  
157 in the combined  $\text{NH}_3$ - $\text{H}_2$  combustion was again shown to reduce the intensity of the premixed  
158 combustion and increase the total combustion duration with respect to the diesel- $\text{NH}_3$ - $\text{H}_2$  combustion.  
159 The highest DGE concentration (i.e. DGE40) even further delayed the peak ROHR, which reduced  
160 therefore the peak cylinder pressure, indicating the decreased combustion temperature. The total  
161 combustion duration (combining the premixed and diffusion phases) and the ROHR in the diffusion  
162 phase increase for both of the gases when applied with the DGE blends. These were based on their  
163 diminished premixed phases, which indicate increased heat was released in the subsequent diffusion  
164 phase compared to the combustion with diesel. And the overall increased heat release duration of  
165 DGE than that of diesel in a broader range of in-cylinder conditions, enhances  $\text{NH}_3$  and  $\text{H}_2$   
166 combustion.

167 The cyclic variation of the combustion was increased with  $\text{NH}_3$  and  $\text{H}_2$  addition, but the  
168 coefficient of variation (COV) of IMEP was kept under 7% for all the conditions. The engine  
169 instability could be derived from the increased incomplete combustion of these gaseous additions  
170 from one cycle to another. This point will be further proved in the following section, using the unburnt  
171 concentration of  $\text{H}_2$  and  $\text{NH}_3$ . The use of DGE improved the engine stability (COV of IMEP was  
172 lower than 3 for all the tested conditions) by its combustion characteristics described earlier i.e. a)  
173 reducing the cylinder pressure and hence the volatile in-cylinder condition through its low  
174 temperature combustion and b) improving the combustions of  $\text{H}_2$  and  $\text{NH}_3$  via its higher ignitability  
175 [19] and overall increased combustion duration.

#### 176 $\text{CO}_2$ and unburned gaseous additions ( $\text{NH}_3$ and $\text{H}_2$ )

177 The trade-off between engine output  $\text{CO}_2$  emissions and the volumetric  $\text{NH}_3$  and  $\text{H}_2$  emissions  
178 under different fuelling conditions are shown in Figure 3a and b respectively. The ammonia measured

179 in the engine exhaust was reduced significantly by the addition of H<sub>2</sub>. This was in accordance with the  
180 H<sub>2</sub> improved NH<sub>3</sub> combustion shown in Figure 2b. However, the unburned NH<sub>3</sub> and H<sub>2</sub> emissions are  
181 still high and other reasons such as NH<sub>3</sub> and H<sub>2</sub> escaping the combustion process during the process of  
182 charge exchange should be also considered.

183 *NH<sub>3</sub> and H<sub>2</sub>*: As it is shown in Figure 3a and b, the presence of DGE also improved the emissions  
184 of NH<sub>3</sub> and H<sub>2</sub> for all the studied cases (diesel-NH<sub>3</sub>, diesel-H<sub>2</sub> and diesel-H<sub>2</sub>-NH<sub>3</sub> combustion). This is  
185 especially noticeable when higher additions of ammonia and hydrogen are used. DGE20 slightly  
186 improved unburnt NH<sub>3</sub> emissions compared to diesel fuelling while the improvement was even further  
187 under the presence of hydrogen (Figure 3a). This is due to the beneficial effect of DGE20 on  
188 hydrogen combustion (Figure 3b) which also enhances NH<sub>3</sub> combustion (synergetic effect) reducing  
189 the unburnt H<sub>2</sub> and NH<sub>3</sub> emissions. Further incorporation of DGE (DGE40) does not statistic  
190 significantly improve further hydrogen combustion, but reduces unburnt NH<sub>3</sub> emissions.

191 The ignition properties of DGE enhanced the combustion pattern (see Figure 2), which improved  
192 also the ammonia and hydrogen combustion and hence reduced the unburnt ammonia and hydrogen  
193 due to, for example, the flame quenching on the chamber walls and the ammonia-air mixture trapped  
194 within the piston-ring crevice. The largest emissions of hydrogen and ammonia were recorded when  
195 DGE was absent and with a co-feeding of NH<sub>3</sub> and H<sub>2</sub> at 14 and 15 l/min. The combined gaseous  
196 addition replaced 29 l/min of the air intake flow, which represented 6% of air reduction in the overall  
197 intake charge. This brought the same dilution effect reducing the in-cylinder oxygen concentration  
198 (similarly to exhaust-gas-recirculation, EGR), which could result in incomplete combustion [20].  
199 Furthermore the increased fuel replacement by high gaseous additions (Figure 1) also affects the  
200 diesel spray characteristics, which were thought to restrict the source of ignition for the gaseous  
201 additions. On the other hand, the low heating value of the DGE blends with respect to diesel results in  
202 a longer injection duration in addition to the longer combustion duration which increase the available  
203 time of the liquid fuel spray and diffusion combustion in the combustion chamber to ignite the  
204 gaseous fuels. Therefore, the fuel-born oxygen brought by DGE and DGE's high ignitability were  
205 inferred to alleviate the i) intake air shortage, ii) poor auto-ignition properties of the gaseous fuels and  
206 iii) reduction of the liquid fuel spray assisting the mixture's ignition and combustion.

207 *CO<sub>2</sub> emissions*: When NH<sub>3</sub> is combusted the CO<sub>2</sub> emissions released to the atmosphere are  
208 significant reduced due to the absence of carbon in the NH<sub>3</sub> molecule, but high unburnt NH<sub>3</sub> was



209 released to the atmosphere resulting in a CO<sub>2</sub>-NH<sub>3</sub> trade off (Figure 3a). The incorporation of H<sub>2</sub> to  
210 diesel-NH<sub>3</sub> combustion enables to simultaneously decrease further the engine output CO<sub>2</sub> and NH<sub>3</sub>  
211 emissions. However, for high H<sub>2</sub> and NH<sub>3</sub> intake concentrations there is some unburnt hydrogen  
212 which is not efficiently combusted (Figure 3b). The use of DGE-diesel blend decreased the  
213 tank-to-wheel (TTW) CO<sub>2</sub> emissions due to the high O/C ratio compared to diesel combustion. The  
214 incorporation of DGE into the liquid diesel fuels enhances the combustion of the carbon free gaseous  
215 fuels (H<sub>2</sub> and NH<sub>3</sub>) and simultaneously decreases the engine output levels of CO<sub>2</sub>, NH<sub>3</sub> and H<sub>2</sub>  
216 released to the atmosphere. The reduction of CO<sub>2</sub> reached approximately 50% of the initial CO<sub>2</sub>  
217 emission recorded from the combustion of diesel fuel only.

218 From the results presented above, it is suggested the large decrease in engine output NH<sub>3</sub>  
219 emissions could be due to a number of phenomena, where the DGE could first enhance the individual  
220 combustions of H<sub>2</sub> and NH<sub>3</sub>, and more importantly, the improved H<sub>2</sub> combustion and its fast flame  
221 speed and propagation subsequently favouring the NH<sub>3</sub>'s combustion, resulting in a synergetic effect  
222 between the gaseous and liquid fuels overall improving the combustion process. This sequenced  
223 pattern is displayed in Figure 4.

#### 224 Brake thermal efficiency

225 The brake thermal efficiencies (BTE) of the engine at different H<sub>2</sub>-NH<sub>3</sub> additions were calculated  
226 using Eq. 1 and are shown in Figure 5.

$$227 \quad \eta = \frac{P_{\text{Brake}}}{(\text{LHV} \times M_f)} \quad \text{Eq. 1}$$

228 Where P<sub>Brake</sub> is the engine brake power, M<sub>f</sub> is the fuel mass flow rate and LHV is the lower  
229 heating value of each fuel and gas (i.e. Diesel, DGE, NH<sub>3</sub> and H<sub>2</sub>).

230 In general, the addition of H<sub>2</sub> and NH<sub>3</sub> into diesel operation decreased the engine thermal  
231 efficiency. This is associated with less efficient combustion of H<sub>2</sub> and NH<sub>3</sub> as described earlier with  
232 reference to Figure 3. Although the NH<sub>3</sub>'s combustion was enhanced by the presence of H<sub>2</sub>, it was not  
233 to the same extend as that of the baseline diesel. For a simple comparison, the hydrocarbon emission  
234 (C<sub>1</sub> based) at the 100% diesel baseline never exceeded 450 ppm at the studied load operation. In  
235 addition, part of the decrease could be also related to the intake air replacement by the H<sub>2</sub> and/or NH<sub>3</sub>  
236 that reduced the overall volumetric efficiency. Apart from the above, H<sub>2</sub> was reported to decrease the  
237 thermal efficiency in diesel combustion due to its higher flame velocity and small quenching distance

238 [21, 22] that increased heat loss to the chamber walls.

239 The DGE addition (DGE40, as an example) was shown to increase the BTE due to the improved  
240 H<sub>2</sub> and NH<sub>3</sub> utilisation as can be proved by the reduced emissions of H<sub>2</sub> and NH<sub>3</sub> under the DGE  
241 addition.

#### 242 Other gaseous emissions

243 *CO and THCs:* Similar trends to CO<sub>2</sub> are also observed for the emission reductions of CO and  
244 unburnt hydrocarbons (Figure 6a and 6b, respectively). The locally enriched fuel-born oxygen  
245 enhanced the complete fuel combustion, suppressing the formation of CO and THC [23]. In addition,  
246 the replacement of carbon based fuels, the more advanced ignition and overall prolonged combustion  
247 duration with the DGE blends (Figure 2b), increased the available time for CO and THC oxidation.  
248 The combustion properties of DGE are believed to support its easier (high CN rating) oxidation even  
249 in the late combustion stage, helping in removing the CO and THC that escaped from the main  
250 combustion events.

251 *NO<sub>x</sub> Emissions:* The PM-NO<sub>x</sub> emissions (NO + NO<sub>2</sub>) trade-off of the diesel and DGE blends  
252 with and without NH<sub>3</sub> and H<sub>2</sub> additions are plotted in Figure 7. Without hydrogen, the NO<sub>x</sub> emission  
253 is shown to increase at small NH<sub>3</sub> additions (up to 3 l/min). When larger quantities of ammonia were  
254 added, the effects of (i) low combustion flame temperature of NH<sub>3</sub> [24] (ii) delayed start of  
255 combustion and consecutively retarded combustion, (iii) lower oxygen availability, all combined  
256 leading in suppressing NO<sub>x</sub> production. As shown in the same plot, when the highest NH<sub>3</sub> flow (14  
257 l/min) was used, the NO<sub>x</sub> emissions became even lower than that of the diesel baseline.

258 On the other hand, the improved NH<sub>3</sub> combustion with hydrogen inevitably enhanced the NO and  
259 NO<sub>2</sub> emission from that of the diesel baseline and is shown to be proportional to the hydrogen level  
260 (Figure 7). Although DGE was demonstrated to improve the NH<sub>3</sub>'s combustion, further decrease in  
261 NO<sub>x</sub> was observed due to the increased DGE presence (with and without the hydrogen addition). As  
262 indicated earlier in the combustion profile (Figure 2), the addition of DGE reduced the cylinder  
263 pressure (i.e. combustion temperature), especially in the premixed combustion phase where the NO<sub>x</sub>  
264 formation is most significant. As a result, NO<sub>x</sub> formation was further suppressed even the hydrogen  
265 promotion effect on NH<sub>3</sub> combustion for the DGE40 blend.

266 On the other hand, N<sub>2</sub>O emissions with the combined fuelling of H<sub>2</sub>, NH<sub>3</sub> to liquid fuel combustion  
267 (for both diesel and DGE blends) were higher than those of just liquid fuel combustion. Around 10-15%

268 of the N<sub>2</sub>O was reduced after the DGE blends being applied. This result needs to be further  
269 investigated in order to control N<sub>2</sub>O emissions due to its high global warming potential.

#### 270 Particulate matter emissions

271 The particulate size distribution and mass concentrations at different levels of DGE, H<sub>2</sub> and NH<sub>3</sub>  
272 are shown in Figure 8a-c and d-f respectively. The total PM emissions expressed in g/kWh are plotted  
273 in the NO<sub>x</sub>-PM trade-off (Figure 7). The particle mass distribution was obtained from the particle  
274 number distribution through a size dependent agglomerate density function as described by Lapuerta  
275 et al. [25]. It has to be noted that only particulates in the range of 10 to 400 nm have been considered  
276 for the total PM estimation. In the case of larger particulates are included the PM emissions would be  
277 higher.

278 Combustion of the DGE blends showed simultaneous reductions in NO<sub>x</sub> and PM emissions with  
279 and without gaseous additions, especially when 40% (v/v) of DGE is incorporated to the diesel fuel  
280 blend. The primary reason was again the oxygen present in the DGE molecule. This would allow  
281 enhanced combustion to take place even in the fuel rich area, which helped to oxidise the PM that  
282 were already formed or improve the oxidation of particles and particle precursors [26-28]. In addition  
283 to that, the prolonged combustion duration (Figure 2) at increased DGE level also provided longer  
284 time for the PM oxidation. Another reason for this PM reduction was based on the fact that DGE is in  
285 the form of ether [11, 29]. Due to its atomic structure of being one oxygen atom bound to two carbon  
286 atoms, the DGE structure was reported to effectively inhibit soot formation, which counts for a large  
287 portion in total PM.

288 After adding hydrogen and ammonia, the mass and number of PM were reduced for both diesel  
289 and DGE blends due to the large replacement of carbon through decreasing the formation of local fuel  
290 rich regions. The individual performance of H<sub>2</sub> and NH<sub>3</sub> are shown to improve at increased DGE level.  
291 This is supported by the reduced H<sub>2</sub> and NH<sub>3</sub> emissions shown earlier, meaning enhanced carbon  
292 replacement were achieved by better H<sub>2</sub> and NH<sub>3</sub> combustion. It is seen that H<sub>2</sub> alone performed better  
293 in PM reduction than that of NH<sub>3</sub>. This is in accordance with the more pronounced premixed phase in  
294 H<sub>2</sub> combustion. The PM emission reduced when simultaneous additions of NH<sub>3</sub> and H<sub>2</sub> were adopted  
295 and decreased further with use of DGE. The number and mass particulate matter size distributions  
296 were decreased across the size spectrum (Figure 8), and hence decreased total mass emissions as  
297 shown in Figure 7. These trends further support the above proposed DGE combustion enhancement

298 (Figure 4), which in turn improved also the PM and NO<sub>x</sub> reduction.

#### 299 **4. Conclusions**

300 Carbon free energy carriers and low carbon renewable fuels such as ammonia and hydrogen can  
301 be used in existing power generation technologies but there are challenges that need to be answered  
302 from the production to storage (especially on-board) and efficiency utilisation. In this research, the  
303 extent of the environmental benefits (i.e. CO<sub>2</sub> and other pollutants) that can be achieved when  
304 synergies in the utilisation of carbon free energy vectors (NH<sub>3</sub> and H<sub>2</sub>) and reduced carbon renewable  
305 fuels such as DGE are identified and assessed. These results are obtained for a research single  
306 cylinder engine. It is believed that quantitative results will depend on engine technology, but general  
307 trends and fundamental understanding of the roles of hydrogen and DGE on NH<sub>3</sub> combustion gained  
308 by this research are also applicable to modern multi-cylinder engines for practical applications. It has  
309 to be noted that the further potential to improve thermal efficiency and CO<sub>2</sub> emissions due to the  
310 possibility of using part of waste exhaust energy in the endothermic reforming process has not been  
311 considered. In addition, only the effects of the carbon-free fuels NH<sub>3</sub> and H<sub>2</sub> have been studied here,  
312 while the effects on combustion and emissions of N<sub>2</sub> produced by ammonia dissociation process have  
313 not been investigated as those effects have been already studied in the literature.

314 The study demonstrates that low carbon renewable fuels such as DGE, can directly impact in  
315 CO<sub>2</sub> emissions but most importantly can be designed to have the suitable properties to enhance the  
316 utilisation of carbon free energy carriers, in this case ammonia and hydrogen. By easing the utilisation  
317 of new environmentally friendly fuels and energy carriers, both CO<sub>2</sub> levels emitted to the atmosphere  
318 (up to 50% demonstrated here on tank-to-wheel bases) as well as other harmful pollutants can be  
319 depleted. The synergies between DGE and carbon-free gaseous fuels have also led in the reduction of  
320 other emissions (i.e. CO and hydrocarbons) and shifted the well-known diesel engine PM and NO<sub>x</sub>  
321 trade-off to lower values. In addition, the combination DGE's molecule oxygen content and good  
322 ignition properties allowed counteracting for the replacement of oxygen part of the air with the  
323 induction of gaseous fuel.

#### 324 **Acknowledgments**

325 The authors would like to thank Johnson Matthey for funding the project. The School of  
326 Mechanical Engineering at the University of Birmingham (UK) is gratefully acknowledged for the

327 PhD School Scholarship to Mr. Wentao Wang. Engineering and Physical Science Research  
328 Council-EPSCRC projects (EP/G038139/1) for supporting the research work. Advantage West  
329 Midlands and the European Regional Development Fund as part of the Science City Research  
330 Alliance Energy Efficiency Project are also acknowledged for supporting the research work.

### 331 **References**

- 332 1. Tsolakis, A.; Megaritis, A., Catalytic exhaust gas fuel reforming for diesel engines—effects of water  
333 addition on hydrogen production and fuel conversion efficiency. *International Journal of Hydrogen Energy* **2004**,  
334 29, (13), 1409-1419.
- 335 2. Wang, W.; Herreros, J. M.; Tsolakis, A.; York, A. P. E., Ammonia as hydrogen carrier for transportation;  
336 investigation of the ammonia exhaust gas fuel reforming. *International Journal of Hydrogen Energy* **2013**, 38,  
337 (23), 9907-9917.
- 338 3. Rees, N. V.; Compton, R. G., Carbon-free energy: a review of ammonia- and hydrazine-based  
339 electrochemical fuel cells. *Energy & Environmental Science* **2011**, 4, (4), 1255-1260.
- 340 4. Zhang, F.; Liu, J.; Yang, W.; Logan, B. E., A thermally regenerative ammonia-based battery for efficient  
341 harvesting of low-grade thermal energy as electrical power. *Energy & Environmental Science* **2015**, 8, (1),  
342 343-349.
- 343 5. Rollinson, A. N.; Jones, J.; Dupont, V.; Twigg, M. V., Urea as a hydrogen carrier: a perspective on its  
344 potential for safe, sustainable and long-term energy supply. *Energy & Environmental Science* **2011**, 4, (4),  
345 1216-1224.
- 346 6. Schuth, F.; Palkovits, R.; Schlogl, R.; Su, D. S., Ammonia as a possible element in an energy infrastructure:  
347 catalysts for ammonia decomposition. *Energy & Environmental Science* **2012**, 5, (4), 6278-6289.
- 348 7. Alam, M.; Goto, S.; Sugiyama, K.; Kajiwara, M.; Mori, M.; Konno, M.; Motohashi, M.; Oyama, K.,  
349 Performance and Emissions of a DI Diesel Engine Operated with LPG and Ignition Improving Additives. *SAE*  
350 *International* **2001**, 2001-01-3680.
- 351 8. Miller Jothi, N. K.; Nagarajan, G.; Renganarayanan, S., LPG fueled diesel engine using diethyl ether with  
352 exhaust gas recirculation. *International Journal of Thermal Sciences* **2008**, 47, (4), 450-457.
- 353 9. Karabektas, M.; Ergen, G.; Hosoz, M., The effects of using diethylether as additive on the performance and  
354 emissions of a diesel engine fuelled with CNG. *Fuel* **2014**, 115, (0), 855-860.
- 355 10. Ryu, K.; Zacharakis-Jutz, G. E.; Kong, S.-C., Performance characteristics of compression-ignition engine  
356 using high concentration of ammonia mixed with dimethyl ether. *Applied Energy* **2014**, 113, (0), 488-499.
- 357 11. Smith, B. L.; Ott, L. S.; Bruno, T. J., Composition-Explicit Distillation Curves of Diesel Fuel with Glycol Ether  
358 and Glycol Ester Oxygenates: Fuel Analysis Metrology to Enable Decreased Particulate Emissions.  
359 *Environmental Science & Technology* **2008**, 42, (20), 7682-7689.
- 360 12. Ito, T.; Ueda, M.; Matsumoto, T.; Kitamura, T.; Senda, J.; Fujimoto, H., Effects of Ambient Gas Conditions  
361 on Ignition and Combustion Process of Oxygenated Fuel Sprays. *SAE International* **2003**, 2003-01-1790.
- 362 13. White, C. M.; Steeper, R. R.; Lutz, A. E., The hydrogen-fueled internal combustion engine: a technical  
363 review. *International Journal of Hydrogen Energy* **2006**, 31, (10), 1292-1305.
- 364 14. Heywood, J., *Internal Combustion Engine Fundamentals*. 2nd ed.; Mc Graw-Hill: New York, 1988.
- 365 15. Saravanan, N.; Nagarajan, G.; Sanjay, G.; Dhanasekaran, C.; Kalaiselvan, K. M., Combustion analysis on a DI  
366 diesel engine with hydrogen in dual fuel mode. *Fuel* **2008**, 87, (17–18), 3591-3599.
- 367 16. Liew, C.; Li, H.; Nuzskowski, J.; Liu, S.; Gatts, T.; Atkinson, R.; Clark, N., An experimental investigation of the

368 combustion process of a heavy-duty diesel engine enriched with H<sub>2</sub>. *International Journal of Hydrogen Energy*  
369 **2010**, 35, (20), 11357-11365.

370 17. Joo, J. M.; Lee, S.; Kwon, O. C., Effects of ammonia substitution on combustion stability limits and NO<sub>x</sub>  
371 emissions of premixed hydrogen–air flames. *International Journal of Hydrogen Energy* **2012**, 37, (8),  
372 6933-6941.

373 18. Li, J.; Huang, H.; Kobayashi, N.; He, Z.; Nagai, Y., Study on using hydrogen and ammonia as fuels:  
374 Combustion characteristics and NO<sub>x</sub> formation. *International Journal of Energy Research* **2014**, 38, (9),  
375 1214-1223.

376 19. Goto, S.; Lee, D.; Wakao, Y.; Honma, H.; Mori, M.; Akasaka, Y.; Hashimoto, K.; Motohashi, M.; Konno, M.,  
377 Development of an LPG DI Diesel Engine Using Cetane Number Enhancing Additives. *SAE International* **1999**,  
378 1999-01-3602.

379 20. Tsolakis, A.; Megaritis, A.; Wyszynski, M. L.; Theinnoi, K., Engine performance and emissions of a diesel  
380 engine operating on diesel-RME (rapeseed methyl ester) blends with EGR (exhaust gas recirculation). *Energy*  
381 **2007**, 32, (11), 2072-2080.

382 21. Shudo, T., Improving thermal efficiency by reducing cooling losses in hydrogen combustion engines.  
383 *International Journal of Hydrogen Energy* **2007**, 32, (17), 4285-4293.

384 22. Shudo, T.; Nabetani, S.; Nakajima, Y., Analysis of the degree of constant volume and cooling loss in a spark  
385 ignition engine fuelled with hydrogen *International Journal of Engine Research* **2001**, 2, (1), 81-92.

386 23. Miyamoto, N.; Ogawa, H.; Nabi, M. N., Approaches to extremely low emissions and efficient diesel  
387 combustion with oxygenated fuels *International Journal of Engine Research* **2000**, 1, (1), 71-85.

388 24. Gross, C. W.; Kong, S.-C., Performance characteristics of a compression-ignition engine using  
389 direct-injection ammonia–DME mixtures. *Fuel* **2013**, 103, (0), 1069-1079.

390 25. Lapuerta, M.; Armas, O.; Gómez, A., Diesel Particle Size Distribution Estimation from Digital Image  
391 Analysis. *Aerosol Science and Technology* **2003**, 37, (4), 369-381.

392 26. Lapuerta, M.; Armas, O.; Herreros, J. M., Emissions from a diesel–bioethanol blend in an automotive  
393 diesel engine. *Fuel* **2008**, 87, (1), 25-31.

394 27. McCormick, R. L.; Ross, J. D.; Graboski, M. S., Effect of Several Oxygenates on Regulated Emissions from  
395 Heavy-Duty Diesel Engines. *Environmental Science & Technology* **1997**, 31, (4), 1144-1150.

396 28. Nord, K. E.; Haupt, D., Reducing the Emission of Particles from a Diesel Engine by Adding an Oxygenate to  
397 the Fuel. *Environmental Science & Technology* **2005**, 39, (16), 6260-6265.

398 29. Westbrook, C. K.; Pitz, W. J.; Curran, H. J., Chemical Kinetic Modeling Study of the Effects of Oxygenated  
399 Hydrocarbons on Soot Emissions from Diesel Engines†. *The Journal of Physical Chemistry A* **2006**, 110, (21),  
400 6912-6922.

401

402

**Table captions**

**Table 1:** Fuel properties of the tested liquid fuel/blend.

**Table 2:** H<sub>2</sub> and NH<sub>3</sub> additions to the engine intake.

**Table 1**

	<b>ULSD</b>	<b>DGE</b>	<b>DGE20</b>	<b>DGE40</b>
<b>Chemical Formula</b>	$C_{14}H_{26.18}$	$C_8H_{18}O_3$	$C_{12.52}H_{24.16}O_{0.74}$	$C_{11.20}H_{22.36}O_{1.40}$
<b>Molar Mass (kg/kmol)</b>	194.18	162	186.24	179.16
<b>Density at 15 °C (kg/m<sup>3</sup>)*</b>	827.1	908	843.3	859.46
<b>LHV (MJ/kg)**</b>	42.99	31.4	40.49	38.10
<b>Cetane Number</b>	53.9	140	-	-
<b>C (wt%)</b>	86.52	59.2	80.67	75.02
<b>H (wt%)</b>	13.48	11.1	12.97	12.48
<b>O (wt%)</b>	0	29.7	6.36	12.50

\* Estimated based on volumetric fraction

\*\* Estimated based on mass fraction



**Table 2**

<b>H<sub>2</sub> (l/min)</b>	<b>20.0</b>				<b>15.0</b>				<b>10.0</b>				<b>0.0</b>			
<b>NH<sub>3</sub> (l/min)</b>	0.0	3.0	7.5	14.0	0.0	3.0	7.5	14.0	0.0	1.0	7.5	14	1.0	3.0	7.5	14.0
<b>H<sub>2</sub>/Reformate</b>	1.0	0.9	0.7	0.6	1.0	0.8	0.7	0.5	1.0	0.9	0.6	0.4	0	0	0	0

## Figure captions

**Figure 1:** Liquid fuel replacement by different H<sub>2</sub> and NH<sub>3</sub> additions.

**Figure 2:** In-cylinder pressure and ROHR of the combustions of diesel and DGE blends with (a) separate additions of NH<sub>3</sub> and H<sub>2</sub> and (b) simultaneous addition of NH<sub>3</sub> and H<sub>2</sub>, the flow rates for NH<sub>3</sub> and H<sub>2</sub> are 14 and 15 l/min respectively.

**Figure 3:** CO<sub>2</sub> and unburned gaseous additions trade-off for (a) NH<sub>3</sub> and (b) H<sub>2</sub> at different fuelling conditions.

**Figure 4** Combustion pattern proposed for DGE enhanced NH<sub>3</sub> and H<sub>2</sub> combustion.

**Figure 5:** Engine brake thermal efficiencies of the combustions of standard diesel and DGE blend with different combinations of H<sub>2</sub> and NH<sub>3</sub>.

**Figure 6:** Carbonaceous gaseous emissions of diesel and DGE blends with different combined additions of H<sub>2</sub> and NH<sub>3</sub> (a) CO and (b) THC.

**Figure 7:** NO<sub>x</sub>-PM trade off.

**Figure 8:** PM number distributions for PM (a) diesel, (b) DGE20 and (c) DGE40 and PM mass distributions for (d) diesel, (e) DGE20 and (f) DGE40

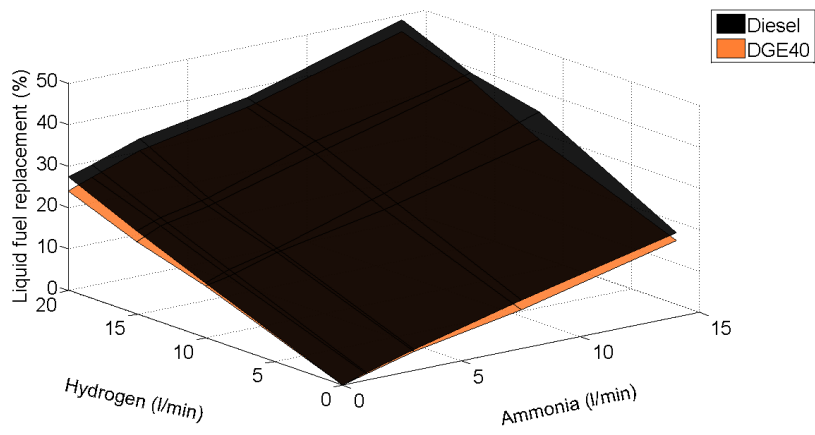


**Figure 1**

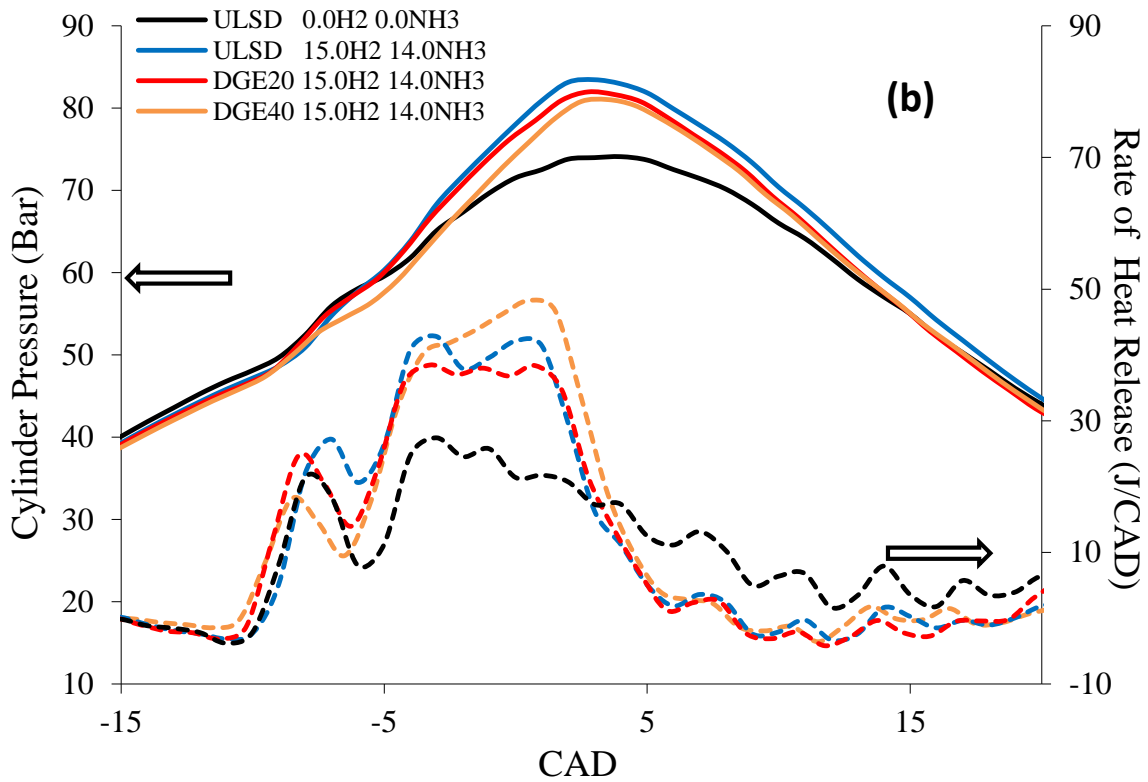
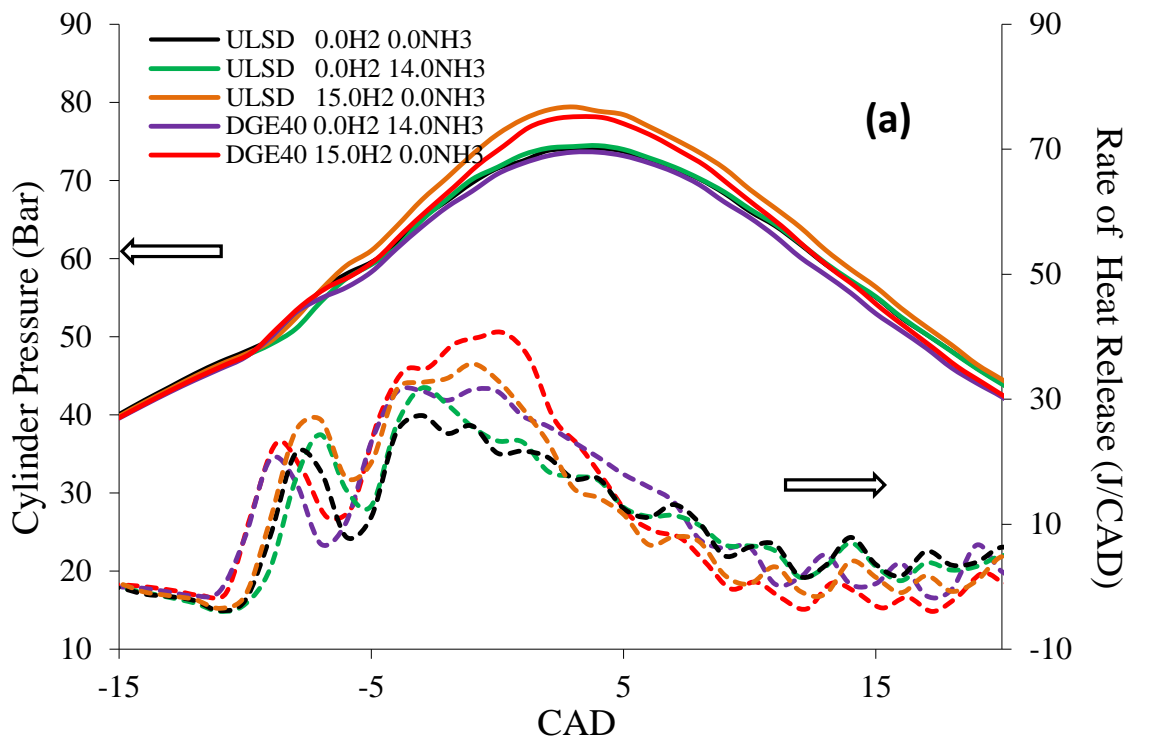


Figure 2

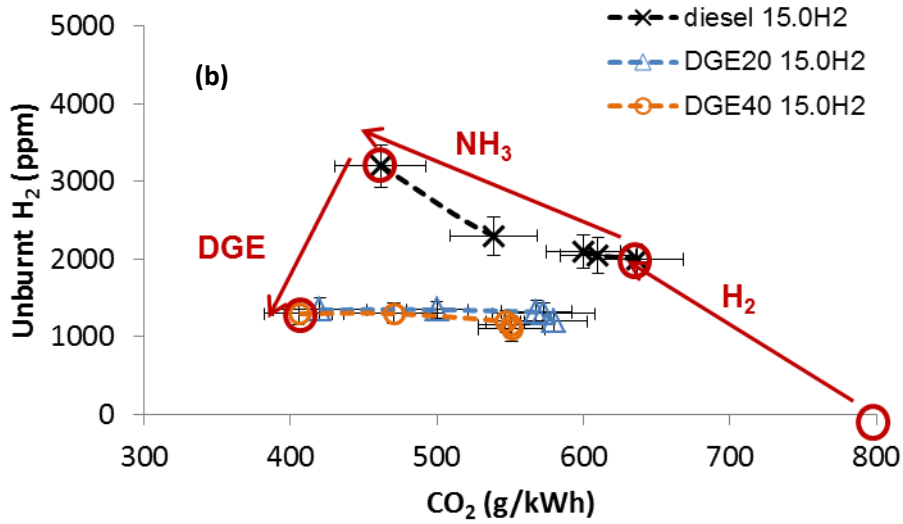
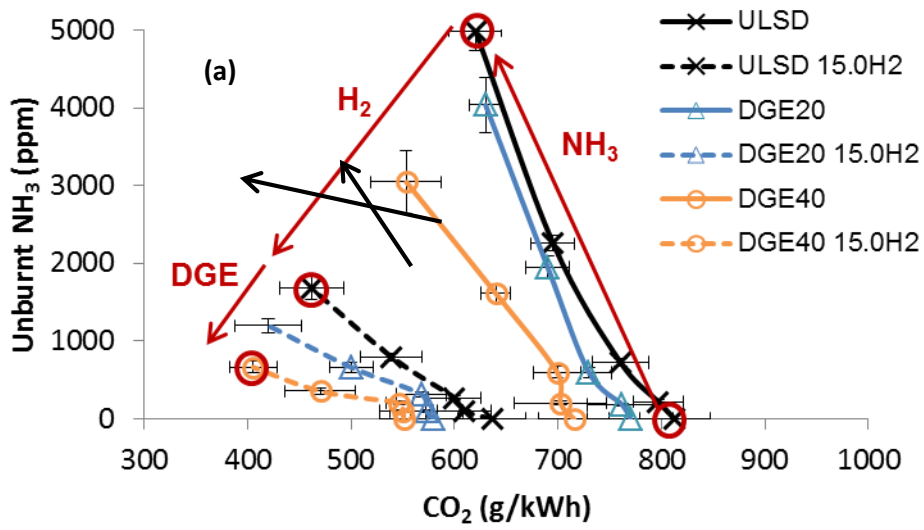


Figure 3

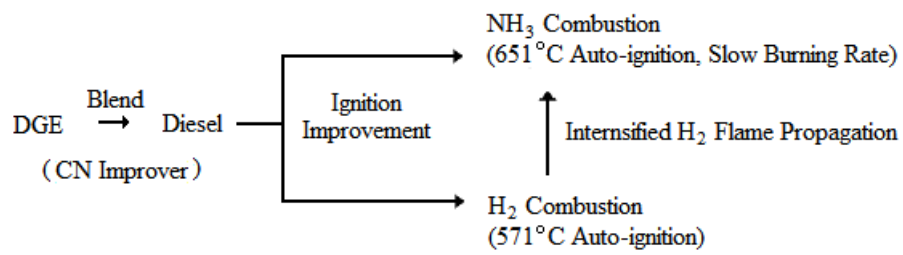
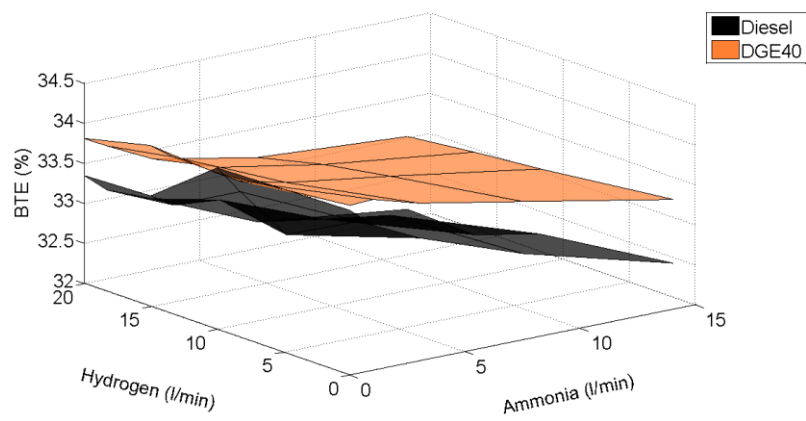
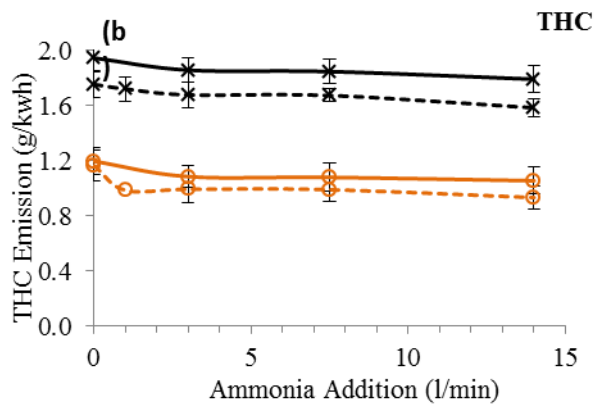
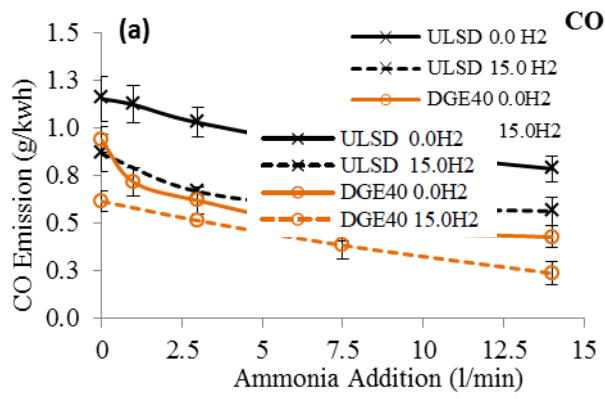


Figure 4



**Figure 5**



**Figure 6**



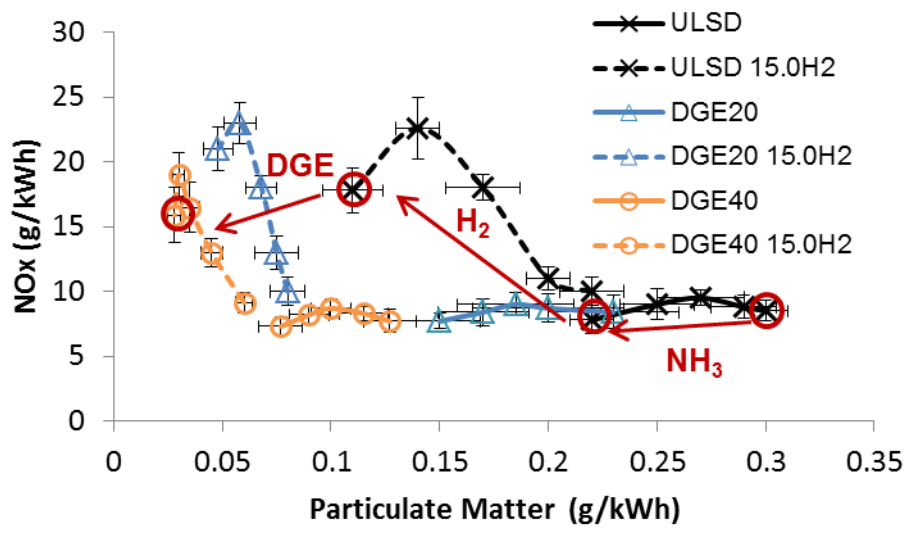
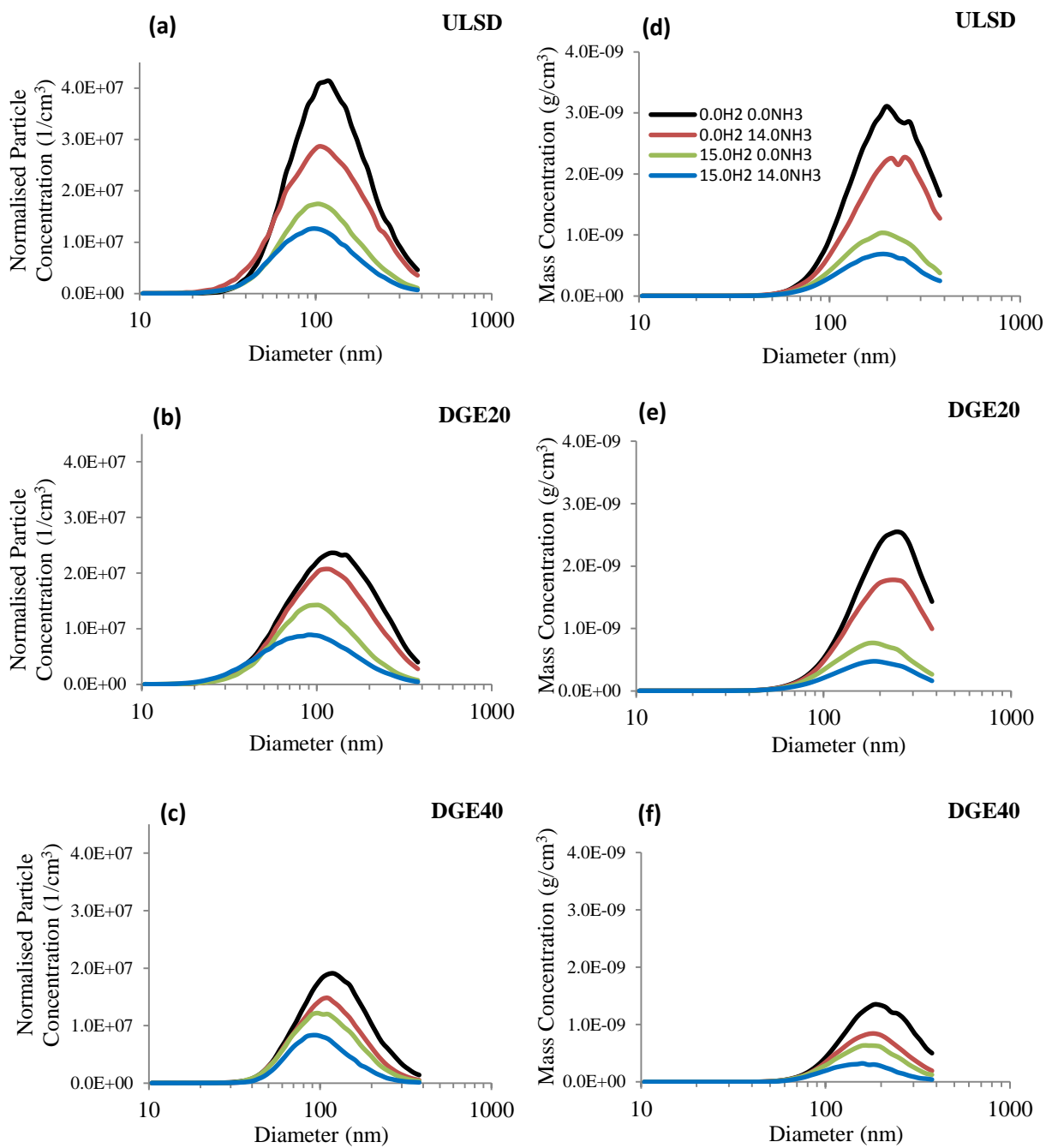


Figure 7



**Figure 8**